OPEN

Genetic Polymorphisms in *SLCO2B1* and *ABCC1* Conjointly Modulate Atorvastatin Intracellular Accumulation in HEK293 Recombinant Cell Lines

Emilia Hoste, MSc,† Adrien Paquot, PharmD,‡ Nadtha Panin, BSc,† Shaleena Horion, MSc,* Halima El Hamdaoui, BSc,* Giulio G. Muccioli, PhD,‡ Vincent Haufroid, PhD,†§ and Laure Elens, PhD*†*

Background: Although atorvastatin (ATV) is well-tolerated, patients may report muscle complaints. These are difficult to predict owing to high interindividual variability. Such side effects are linked to intramuscular accumulation of ATV. This study aimed to investigate the relative role of transporters expressed in muscle tissue in promoting or limiting drug access to cells. The impact of common single nucleotide polymorphisms (SNPs) in *SLCO2B1* coding for OATP2B1 and *ABCC1* coding for MRP1 on ATV transport was also evaluated.

Methods: HEK293 cells were stably transfected with plasmids containing cDNA encoding wild-type or variant *SLCO2B1* and/or *ABCC1* to generate single and double stable transfectant HEK293 recombinant models overexpressing variant or wild-type OATP2B1 (influx) and/or MRP1 (efflux) proteins. Variant plasmids were generated by site-directed mutagenesis. Expression analyses were performed to validate recombinant models. Accumulation and efflux experiments were performed at different concentrations. ATV was quantified by LC-MS/MS, and kinetic parameters were compared between single and double HEK transfectants expressing wild-type and variant proteins.

Results: The results confirm the involvement of OATP2B1 and MRP1 in ATV cellular transport because it was demonstrated that intracellular accumulation of ATV was boosted by OATP2B1 overexpression, whereas ATV accumulation was decreased by MRP1 overexpression. In double transfectants, it was observed that increased ATV intracellular accumulation driven by OATP2B1 influx was partially counteracted by MRP1 efflux. The c.935G > A SNP in *SLCO2B1* was associated with decreased ATV OATP2B1-mediated influx, whereas the c.2012G > T SNP in *ABCC1* seemed to increase MRP1 efflux activity against ATV.

Conclusions: Intracellular ATV accumulation is regulated by OATP2B1 and MRP1 transporters, whose functionality is modulated by natural genetic variants. This is significant because it may play a role in ATV muscle side-effect susceptibility.

Key Words: atorvastatin, pharmacogenetic, influx and efflux transporters, adverse drug reactions

(*Ther Drug Monit* 2023;45:400–408)

INTRODUCTION

Atorvastatin (ATV), an HMG-CoA reductase inhibitor, commercialized under the name of statins, has proven its efficacy in reducing increased blood levels of low-density lipoprotein (LDL) cholesterol and limiting the risk of cardiovascular disease.[1,2] Although generally well tolerated, 5%–10% of patients may suffer from muscle complaints, a relatively uncomfortable side effect that can eventually lead to spontaneous poor patient compliance.[3–5] As an HMG-CoA reductase inhibitor, ATV competitively inhibits the mevalonate pathway implicated in cholesterol synthesis.[6] Although ATV-mediated HMG-CoA reductase inhibition is related to its effect on cholesterol synthesis, it is believed to also account for its adverse effects, among which are muscular

Received for publication May 24, 2022; accepted August 15, 2022.

From the *Integrated PharmacoMetrics, PharmacoGenomics and Pharmacokinetics, Louvain Drug Research Institute (LDRI), Université Catholique de Louvain (UCLouvain); †Louvain Center for Toxicology and Applied Pharmacology, Institut de Recherche Expérimentale et Clinique (IREC), Université Catholique de Louvain (UCLouvain); ‡Bioanalysis and Pharmacology of Bioactive Lipids, Louvain Drug Research Institute (LDRI), Université Catholique de Louvain (UCLouvain); and §Department of Clinical Chemistry, Cliniques Universitaires Saint-Luc, Brussels, Belgium.

Supported by Fonds pour la Formation à la Recherche dans l'Industrie et dans l'Agriculture (FRIA) under the Grant Number FC33437 to E. Hoste, and by grants from the Fonds national de la Recherche scientifique [FRS-FNRS] (Grants J018317 and J006920).

E. Hoste, V. Haufroid, and L. Elens designed the research; E. Hoste, N. Panin, and H. El Hamdaoui conducted the experiments; E. Hoste, N. Panin, and S. Horion designed the cell models; A. Paquot and G.G. Muccioli performed the HPLC/MS–MS analysis; E. Hoste, V. Haufroid, and L. Elens drafted the manuscript; all authors reviewed and approved the final version of the document.

The authors declare no conflict of interest.

Supplemental digital content is available for this article. Direct URL citations appear in the printed text and are provided in the HTML and PDF versions of this article on the journal's Web site (www.drug-monitoring.com).

All experimental data generated and/or analyzed during the study are available from the corresponding author on reasonable request. Observations related to rs12422149 and rs45511401 SNPs have been deposited in ClinVAR under accession numbers SCV002499648 and SCV002499649.

Correspondence: Laure Elens, PhD, Integrated PharmacoMetrics, PharmacoGenomics and PharmacoKinetics (PMGK) Research Group, Louvain Drug Research Institute (LDRI), Université Catholique de Louvain (UCLouvain). Avenue Emmanuel Mounier 72, B1.72.02 Brussels, Belgium (e-mail: laure.elens@uclouvain.be).

complaints. In fact, the ATV-mediated inhibition of the mevalonate pathway and the consequent downstream metabolite depletion leads to a joint reduction of their respective physiological activities which could possibly explain the ATV-related muscular side effects.[7] ATV-mediated HMG-CoA reductase inhibition and the resulting metabolite depletion are known to be dose-dependent.[1] This dose-dependent response suggests that understanding ATV intracellular pharmacokinetics (PK) and the factors affecting it is necessary to unravel the reasons for treatment response variabilities and susceptibility to muscle side effects. In particular, the fact that statin-associated muscle symptoms are specific to skeletal muscle tissue, and dose and drug potency dependent,[8–10] provides a rationale for exploring the importance of factors affecting intramyocyte concentrations. ATV can enter myocytes where toxicity occurs through passive diffusion. However, some data also suggest that active transport is a preponderant mechanism.[11] The activity of transporters expressed in skeletal muscle tissue is assumed to modulate drug concentrations directly within myocytes through both drug efflux and influx. Among the efflux transporters implicated in ATV PK, MRP1, encoded by *ABCC1* (ATP-binding cassette subfamily C, member 1), is one of the most expressed, whereas OATP2B1, encoded by *SLCO2B1* (solute carrier organic anion subfamily 2B, member 1) is, to the best of our knowledge, the only drug influx transporter involved in ATV transport and expressed in skeletal muscle tissues.[12] This suggests that these transporters play a role in protecting or sensitizing myocytes from statin toxicity. However, the correlation between transporter activity and ATV cellular disposition has been poorly explored. Elucidating the potential impact of functional single nucleotide polymorphisms (SNPs) on the role of these transporters in driving the drug across membranes and determining drug cellular accumulation may explain the interindividual differences in the risks of muscle side effects. *ABCC1* is located on chromosome 16p13.11 and contains 34 exons (NG_028268.2). This efflux transporter transports various molecules such as ions, glutathione, or xenobiotics.[13] *ABCC1* expression is relatively ubiquitous. However, its expression is significant in the lungs, on the basolateral membranes of proximal renal tubular cells, and epithelial cells of the small intestine. *ABCC1* is not expressed in the liver.[14] *ABCC1* is highly polymorphic. Among others, the rs45511401 (c.2012G > T, Gly671Val) SNP is a nonsynonymous coding SNP located close to the first nucleotide-binding domain of the protein.[15] OATP2B1 is an influx drug carrier that transports endogenous (eg, estrone-3-sulfate and pregnenolone sulfate) and exogenous (eg, ATV and rosuvastatin) substrates. Its coding gene (*SLCO2B1*) is located on chromosome 11q13.4, which contains 16 exons (NG_027921.1).[16] This influx transporter is mainly expressed on the basolateral hepatic membranes, facilitating the extraction of endogenous substrates and drugs from the blood to the hepatocyte for further metabolization.[17,18] It is also expressed in the skeletal muscle tissue, blood–brain barrier, kidney, small intestine, and, to a lesser extent, placenta.[19] Because the protein is not very well characterized, little data are available. However, the nonsynonymous SNP rs12422149 (c.935G > A, Arg312Gln) in *SLCO2B1* has been associated with increased simvastatin plasma levels and reduced rosuvastatin efficiency, suggesting a significant effect of this SNP on the PK of its substrates.[20,21] However, to date, no data on ATV are available.

Both polymorphisms are commonly found in the general population (Table 1). The minor allele frequency of rs45511401 in *ABCC1* is higher in the European population (4.6%) than that in the American (2%), South Asian (1.1%), and African (0.5%) populations, with a global minor allelic frequency of approximately 2%. The minor allele frequency of rs12422149 in *SLCO2B1* is higher globally (21%), with a very high frequency in American (36.5%) and Southeast Asian populations (26.3% and 32%, respectively) and a lower frequency in African and European populations (9.2% and 9.5%, respectively).[22,23]

The goal of this study was to assess the activity of both transporters and the functional effects of 2 common nonsynonymous coding SNPs on ATV cellular transport. In this context, in vitro recombinant models overexpressing the transporters either separately (single transfectants) or simultaneously (double transfectants) were developed by stably transfecting HEK293 cells.

MATERIALS AND METHODS

Materials

Atorvastatin (ATV) was purchased from Pfizer (New York, NY), and the d5-ATV calcium salt was purchased from Alsachim (CAS number:222,412-82-0). Gentamicin (G418), hygromycin B, dimethyl sulfoxide, ampicillin, and kanamycin were purchased from Sigma-Aldrich (St. Louis, MO).

Cell Culture

Control and transfected human embryonic kidney cells (HEK293, ATCC N°CRL-1573) were grown in Dulbecco modified Eagle medium with high glucose, L-glutamine, and sodium pyruvate (DMEM GIBCO) supplemented with 10% (vol/vol) fetal bovine serum and 1% (vol/vol) penicillin–streptomycin (Thermo Fisher Scientific, Waltham, MA). The cells were cultured at 37°C and 5% CO_2. For reculturing, the cells were detached with enzyme-free cell dissociation buffer (Thermo Fisher Scientific).

TABLE 1. Minor Allele Frequency Among Ethnicities for rs45511401 in *ABCC1* and rs12422149 in *SLCO2B1* According to Ensembl.org

rs45511401 in *ABCC1*		**rs12422149 in *SLCO2B1***	
Global	0.015	Global	0.210
European	0.046	European	0.095
American	0.020	American	0.365
African	0.005	African	0.092
South Asian	0.011	South Asian	0.263
East Asian	0	East Asian	0.320

Generation of *SLCO2B1*$_{935G}$ and *SLCO2B1*$_{935A}$ Plasmids

The expression vector pCMV-V-OFPSpark, which encodes the wild-type (WT) OATP2B1 protein *(SLCO2B1*$_{935G}$*)*, and a C-terminal fluorescent red tag (OFPSpark) were purchased from Bio-Connect Life Sciences (cat. HG18756-ACR; Huissen, the Netherlands). The construct contained sequences coding for kanamycin and hygromycin B resistance genes, allowing for further bacterial and eukaryotic cell selection, respectively. The variant plasmid expressing *SLCO2B1*$_{935A}$ (rs12422149) was generated by site-directed mutagenesis by polymerase chain reaction (iCycler iQ; BioRad, Hercules, CA) using the Phusion Site-Directed Mutagenesis Kit (Waltham, MA) following the manufacturer's protocol. The back-to-tail primers phosphorylated in 5′-OH, including the point mutation, were 5′-CAG TTT CGG CAA AAG GTC TTA G-3′ (forward) and 5′-AAG CTC ACG TTT TTC CTT G-3′ (reverse) and were purchased from Eurofins Scientific société européenne (Ebersberg, Germany). Plasmid transformation and amplification were performed in dH5$_{\alpha}$ *Escherichia coli* strains using heat shock. The product was purified using a PureLink HiPure Plasmid Filter Maxiprep (Thermo Fisher Scientific, Waltham, MA). The amplicon was sequenced using a Sanger method (Eurofins, Germany) to confirm the introduction of the point mutation c.935G > A into the coding nucleotide sequence of *SLCO2B1* (see **Supplemental Data, Figure S1a, b**, **Supplemental Digital Content 1**, http://links.lww.com/TDM/A619).

Generation of *ABCC1*$_{2012G}$ and *ABCC1*$_{2012T}$ Plasmids

The expression vector pcDNA3.1-eGFP that was kindly provided by Dr. Susan Cole[15] codes for WT MRP1 protein (ABCC1$_{2012G}$) with a green fluorescent tag (GFP). The construct contained sequences coding for ampicillin and gentamicin resistance genes, allowing for further bacterial and eukaryotic cell selection, respectively. For *SLCO2B1*, a variant plasmid expressing *ABCC1*$_{2012T}$ (rs45511401) was generated by site-directed mutagenesis by polymerase chain reaction using the Phusion Site-Directed Mutagenesis Kit. The back-to-tail primers phosphorylated at the 5′-OH, including the point mutation, were 5′-ATC CCC GAA GTT GCT TTG GTG-3′ (forward) and 5′-GGA GAA GGT GAT GCC ATT C-3′ (reverse). The product was amplified and purified under the same conditions as described previously, and the variant was successfully introduced into the coding sequence of *ABCC1* (see **Supplemental Data, Figure S1c, d**, **Supplemental Digital Content 1**, http://links.lww.com/TDM/A619).

Generation of Stable Recombinant Cell Lines

For single transfectants, overexpressing either WT or the variant (var) OATP2B1 protein HEK$_{OATP2B1WT}$ and HEK$_{OATP2B1var}$, 5×10^5 HEK293 cells/well were seeded in 12-well plates the day before transfection with the Lipofectamine 3000 Transfection Kit (Invitrogen, Carlsbad, CA) with 1.25 mcg of plasmid DNA (either *SLCO2B1*$_{935G}$ or *SLCO2B1*$_{935A}$ plasmids). The same method was used to obtain HEK$_{MRP1WT}$ and HEK$_{MRP1var}$ single transfectants. For the double transfectants, 1×10^6 cells overexpressing 1 of the 2 proteins (HEK$_{OATP2B1WT}$ or HEK$_{OATP2B1var}$) were cultured in 6-well plates 1 day before lipofection. Transfection was then achieved using 2.5 mcg of plasmid DNA per well (either *ABCC1*$_{2012G}$ or *ABCC1*$_{2012T}$ plasmids). The antibiotic selection was performed 72 hours postlipofection with hygromycin B and G418 at a final concentration of 0.5 mg/mL and 1 mg/mL to select cells that stably expressed OATP2B1 and/or MRP1 proteins, respectively. Resistant strains were reseeded after 14 days for future development and sorted by flow cytometry.

Double transfectant models were renamed thereafter, with the model overexpressing both WT transporters (HEK$_{OATP2B1WT-MRP1WT}$); the model overexpressing *SLCO2B1* WT and *ABCC1* variant, HEK$_{OATP2B1WT-MRP1var}$; and the model overexpressing *SLCO2B1* variant and *ABCC1* WT, HEK$_{OATP2B1var-MRP1WT}$. Based on the relatively low frequency of polymorphisms in the population, the impact of both variants in the double transfectant model HEK$_{OATP2B1var-MRP1var}$ was not investigated (the theoretical frequency of the combination is 0.66%).

Characterization of OATP2B1 and MRP1 Protein Expression

Flow Cytometry

The cells were detached, counted, and centrifuged at 400*g* for 5 minutes at 4°C on the day of the experiment. The supernatant was discarded, and the cell pellet was resuspended in 2 mL of sterile fluorescence activated cell sorter (FACS) buffer (Dulbecco PBS, 1% (vol/vol) decomposed fetal bovine serum, 0.001mol/L EDTA [Thermo Fisher Scientific]). Cells were washed twice and resuspended in FACS buffer for analysis with a BD-FACS Verse or sorting with a BD FACSAria III (BD Biosciences, NJ). OFPSpark (red OATP2B1) and green fluorescence (eGFP) (green MRP1) were excited with a blue laser (488 nm) using bandpass filters band pass 586/42 and 527/32, respectively. Raw data were analyzed using FlowJo version 10.8.1 (Ashland, OR). Because fluorescent OFPSpark and eGFP emission spectra partially overlapped, the data were compensated using FlowJo.

All the generated recombinant models were sorted using fluorescence parameters gated at the same level of intensity to ensure similar protein expression. Sorted cells were reseeded in 12-well plates with adequate selective antibiotic concentrations to allow for growth expansion.

Inverted Fluorescence Microscope

Cells were seeded in Ibidi 4 chambers pH+ μ-slide (Gräfelfing, Germany) 48 hours before microscopic analysis using Zeiss Observer Z1 (Zeiss, Germany). The fluorescence signals were obtained using a Zeiss Colibri 7 LED light source. Red fluorescence (OFPSpark) emitted by the tag attached to OATP2B1 was observed with a yellow LED at an excitation wavelength of 555 nm and an emission quadrature bandpass 582/30. EGFP emitted by the tag attached to MRP1 was observed with a blue LED at an excitation wavelength of 475 nm and an emission quadrature bandpass 514/30. Images were captured with a Zeiss Axiocam 506 mono and processed using Zeiss Zen 2 lite.

Characterization of OATP2B1 and MRP1 Activity

Atorvastatin Intracellular Accumulation and Efflux Kinetics

The day before the accumulation assay, the cells (3×10^5) were seeded in 24-well plates coated with poly-L-lysine (Sigma-Aldrich), reaching a confluence of ~90% the next day. On the day of the experiment, 50 μL of each well was removed and 50 μL of freshly diluted ATV solution was added. For drug accumulation, cells were incubated for 120 minutes with increasing ATV concentrations (0, 50, 75, 100, 150, and 500 nM), whereas a concentration of 75 nM was selected for efflux kinetics. All experiments were performed at least twice (N = 2) in triplicate (n = 3). After ATV incubation at 37°C with 5% CO_2 saturation, the plates were centrifuged (Eppendorf 417 R) at 400*g* for 5 minutes at 4°C and the supernatant was discarded. Cells were washed 3 times with 500 μL ice-cold D-PBS and either recovered for accumulation experiments or allowed to efflux in drug-free medium for 30, 60, 120, and 300 minutes. The cells were finally resuspended in 500 μL of D-PBS supplemented with 0.001mol/L EDTA, transferred to a 1.5 mL Eppendorf (Hamburg, Germany), and centrifuged at 400*g* for 5 minutes at 4°C. The supernatant was discarded, and the cell pellet was stored at −20°C for further extraction. For efflux kinetics, aliquots of media (500 μL) were collected at each time point to quantify the fraction of drug effluxed and the cell pellet collected using the method described previously. The efflux ratio was calculated by normalizing the amount of effluxed ATV in the medium at the time points (30, 60, 120, or 300 minutes) on the intracellular amount accumulated at the start of the efflux period (ie, after 2 hours of accumulation).

Atorvastatin Extraction and Quantification

The thawed cell pellets were resuspended in 100 μL of an extraction solvent consisting of a mixture of methanol–water (60:40, v/v) and d5-ATV at a final concentration of 5 nM. The samples were vortexed, sonicated for 10 minutes, and centrifuged for 5 minutes at 10,600*g* at room temperature (20°C). The cell pellets were stored at −20°C for protein assay, and supernatants were transferred to an injection vial and dried under nitrogen flow. The residue was resuspended in 30 μL of methanol before injection into the HPLC-MS/MS system. For ATV quantification, 500 μL of media was added to 1.2 mL of ice-cold acetone supplemented with d5-ATV at a final concentration of 5 nM. The mixture was vigorously vortexed, stored at −20°C for 2 hours, and then centrifuged at 10,600*g* for 10 minutes. The supernatant was then evaporated and resuspended in methanol. Each extract (5 μL) was injected into an HPLC-MS/MS system (Xevo TQ-S, Waters, Milford, MA). Analyte separation was performed using a gradient between mobile phase A (MeOH-H_2O (75:25) with 0.1% (v/v) acetic acid) and mobile phase B (MeOH with 0.1% (v/v) acetic acid) and a ultra performance liquid chromatography column [Ascentis Express C18 column (2.7 μm, 150 × 4 mm)] equipped with a precolumn. For MS/MS detection, ionized compounds were generated using an electrospray source operated in positive mode. Detection was performed in the multiple reaction monitoring mode using the quantification transitions 564.3 → 440.3 for d5-ATV and 559.2 → 440.2 ATV. Calibration curves were established between 0.5 and 1000 fmol ATV on the column. In addition, in each run of ATV quantification, we screened our samples for ortho-hydroxy-atorvastatin and para-hydroxy-atorvastatin (575.2 > 440.2) and for atorvastatin lactone (541.2 > 448.2).[4] In all cases, metabolite levels were below the respective detection limits (0.4 and 0.5 fmol for para-OH-ATV and ortho-OH-ATV, respectively, and 0.375 fmol for ATV lactone), suggesting that the spontaneous conversion of the acid form is very limited in our in vitro system and cannot explain the observed differences. Data analysis was performed using the MassLynx software (waters). ATV concentrations were normalized to total protein content.

Protein Normalization and Statistical Analysis

The protein assay was performed in triplicate for each sample with thawed cell pellets using a DC Protein Assay (BioRad, Hercules, CA).

Graphs and statistical analyses were performed using GraphPad Prism version 8.4.2. To assess the impact of transporters on the intracellular accumulation of ATV, 2-way analysis of variance was used to evaluate the impact of 2 independent factors, that is, ATV incubation concentration (accumulation experiment) or efflux time (efflux kinetics), and the cell lines. Bonferroni post hoc tests were performed for multiple comparisons to determine which means differed from the others. In all cases, the results were considered significant when the P value was < 0.05.

RESULTS

Generation of Stable *SLCO2B1*$_{935G}$ and *SLCO2B1*$_{935A}$ Overexpressing Cell Lines and Characterization of OATP2B1 Expression

After transfection of HEK293 cells with pCMV-V-OFPSpark containing the coding sequence *SLCO2B1*$_{935G}$ or *SLCO2B1*$_{935A}$, similar OATP2B1 expression was ensured by sorting the cells using a fluorescence activated cell system (FACS) gated on the same level of fluorescence intensity.

The expression levels of OATP2B1 were examined using fluorescence microscopy. The results confirmed that the recombinant cell lines $HEK_{OATP2B1WT}$ and $HEK_{OATP2B1var}$ overexpressed OATP2B1 influx protein. Bright red fluorescence of the overexpressing cells was observed in $HEK_{OATP2B1WT}$ and variant, whereas no fluorescent signal was observed for the control cells (HEK_{CTRL}) (Fig. 1A). Furthermore, a strong encircling fluorescent signal was observed, indicating the dominant location of transporters in the membrane.

Generation of Stable *SLCO2B1*$_{935G/A}$ and *ABCC1*$_{2012G/T}$ Double Transfectant Cell Lines and Characterization of Their Protein Expression Levels

As described in the Materials and Methods section, double transfectants were generated by transfecting cells stably expressing OATP2B1 with pcDNA3.1-eGFP *ABCC1* expression vectors (either WT or variant). For single transfectants, similar protein expression was ensured by sorting the cells by FACS gating at the same level of fluorescence intensity. This

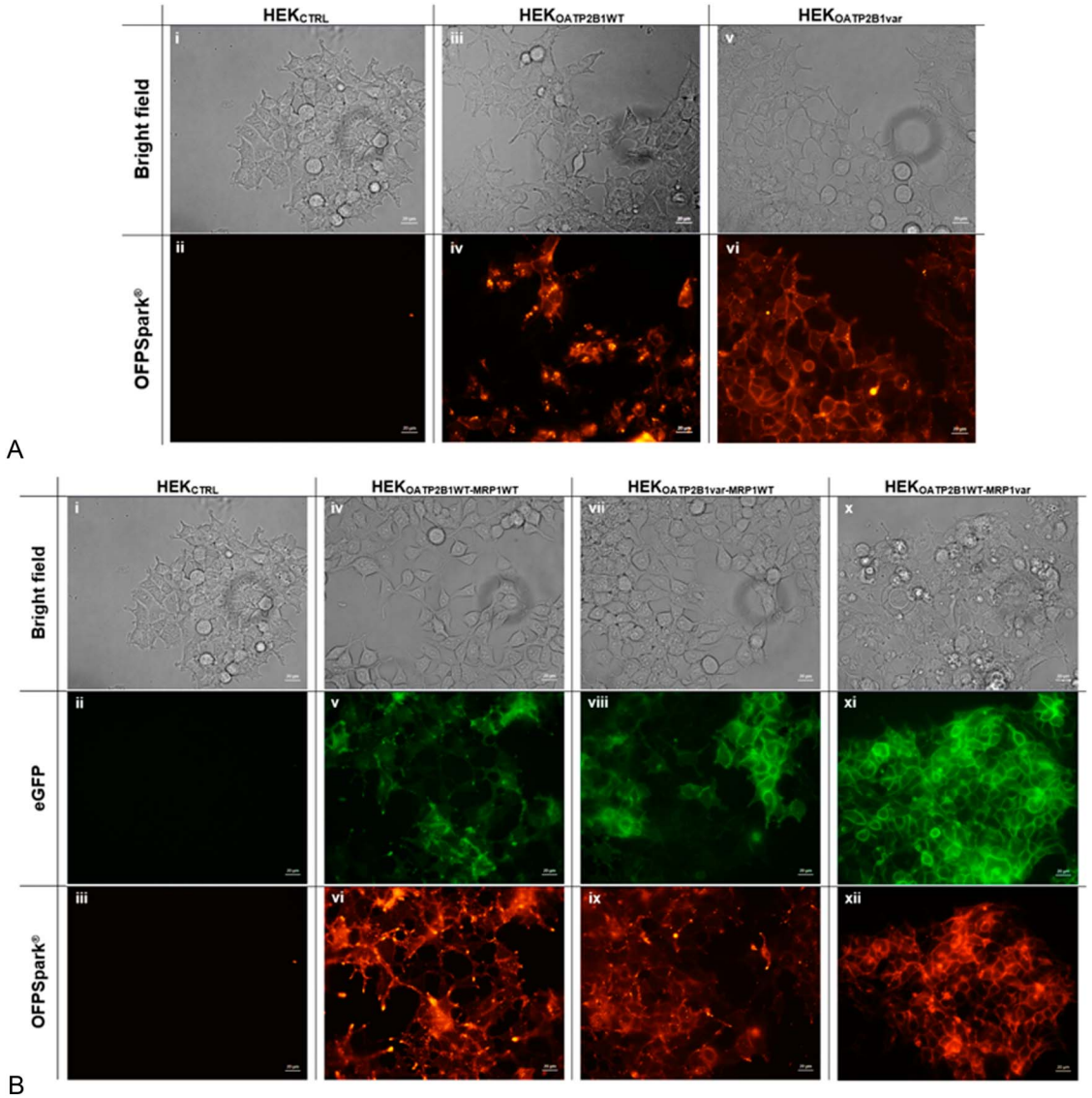

FIGURE 1. Fluorescence microscopy in (A) single transfectant models (i, ii) HEK_{CTRL}, (iii, iv) recombinant $HEK_{OATP2B1WT,}$ and (v, vi) recombinant $HEK_{OATP2B1var}$ in bright field above and in red OFPSpark detection below and fluorescence microscopy in (B) double transfectant models (i–iii) HEK_{CTRL}, (iv–vi) recombinant $HEK_{OATP2B1WT\text{-}MRP1WT}$, (vii–ix) recombinant $HEK_{OATP2B1var\text{-}MRP1WT}$, and (x–xii) recombinant $HEK_{OATP2B1WT\text{-}MRP1var}$ in bright field above, in green eGFP detection centered, and in red OFPSpark detection below.

was confirmed by inverted fluorescence microscopy, where all double transfectants expressed green and red fluorescence when compared with HEK_{CTRL} cells (Fig. 1B). This observation confirmed that both the influx and efflux proteins were overexpressed in the double transfectant cell models.

Effect of *SLCO2B1*$_{935G}$ versus *SLCO2B1*$_{935A}$ Overexpression on ATV Intracellular Accumulation

The results presented in Figure 2 compare the intracellular accumulation of ATV in $HEK_{OATP2B1WT}$, $HEK_{OATP2B1var}$, and HEK_{CTRL} cells. After 2 hours of drug incubation, ATV cellular content was significantly increased in $HEK_{OATP2B1WT}$ cells compared with $HEK293_{CTRL}$ cells from 25 nM onward ($*P < 0.05$ at 25 nM, $**P < 0.01$ at 50 nM, $****P < 0.0001$ from 75 nM of ATV). Interestingly, $HEK_{OATP2B1var}$ showed reduced ATV accumulation compared to its WT counterpart, and the difference was significant at 150 nM and 500 nM. ($\#\#\#P < 0.01$ at 150 nM and $\#\#\#\#\#P < 0.001$ at 500 nM).

Effect of *SLCO2B1*$_{935G/A}$ and *ABCC1*$_{2012G/T}$ Co-expression on the Intracellular Accumulation of ATV

After 2 hours of incubation with increasing concentrations of ATV, the percentage accumulation in HEK293

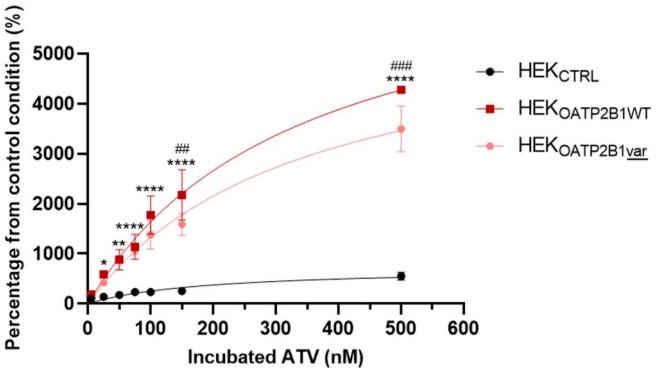

FIGURE 2. ATV accumulation experiment represented in percentage from the control condition (ATV accumulation in HEK_{CTRL} at the lowest concentration) in single transfectant models $HEK_{OATP2B1WT}$ and $HEK_{OATP2B1var}$ compared with the control cells HEK_{CTRL} (*$P < 0.05$, **$P < 0.01$, ****$P < 0.0001$ $HEK_{OATP2B1WT}$ compared with HEK_{CTRL} and ##$P < 0.01$, ###$P < 0.001$ $HEK_{OATP2B1var}$ compared with HEK_{CTRL}).

control cells was lower than that in all other cell lines (Figs. 3A, B). By contrast, intracellular accumulation in the single transfectant $HEK_{OATP2B1WT}$ cells was higher than that in all other cell lines, regardless of the conditions.

Interestingly, MRP1WT activity reduced the increased accumulation generated by the OATP2B1WT influx. Indeed, intracellular ATV accumulation in $HEK_{OATPWT-MRP1WT}$ double transfectant was significantly lower than that in $HEK_{OATP2B1WT}$ but still significantly higher than that in HEK_{CTRL} cells (*$P < 0.05$ at 75 nM and ****$P < 0.0001$ from 100 nM ATV) (Fig. 3A).

Moreover, the expression of one of the 2 variant proteins in $HEK_{OATP2B1var-MRP1WT}$ or $HEK_{OATP2B1WT-MRP1var}$ significantly reduced intracellular ATV accumulation compared with that in WT double transfectant model $HEK_{OATP2B1WT-MRP1WT}$ (**$P < 0.01$, 75 nM, ***$P = 0.001$ at 100 nM and ****$P < 0.0001$ from 150 nM for $HEK_{OATP2B1var-MRP1WT}$ and #####$P < 0.0001$ from 100 nM ATV for $HEK_{OATP2B1WT-MRP1var}$) (Fig. 3B).

Effect of *ABCC1*$_{2012G/T}$ and *SLCO2B1*$_{935G/A}$ Coexpression on Atorvastatin Efflux

As expected, HEK_{CTRL} cells showed weaker efflux ratio compared with the 3 tested double transfected cell lines (Fig. 4). After 60 minutes of efflux time, a nonsignificant trend ($P > 0.05$) of a higher efflux ratio for the double transfectant model $HEK_{OATP2B1WT-MRP1var}$ was observed compared with cell lines expressing WT MRP1 ($HEK_{OATP2B1WT-MRP1WT}$ and $HEK_{OATP2B1var-MRP1WT}$). Both cell lines expressing MRP1WT were characterized by an intermediate efflux ratio. Interestingly, the OATP2B1 variant did not affect the efflux ratio. This observation is consistent with the fact that OATP2B1 is an influx transporter and is thus expected to affect accumulation after 120 minutes rather than on drug efflux.

DISCUSSION

Increasing evidence supports the involvement of transporters in the biodistribution of drugs. However, little information is available on the local cellular consequences of their expression and on the functional relevance of SNPs in explaining the differences in intracellular drug accumulation. In this study, we generated different recombinant model overexpressing proteins assumed to play an important role in the local PK of ATV. In fact, OATP2B1 and MRP1 are both expressed at the skeletal muscle tissue membrane where ATV dose-dependent toxicity is exerted.[12] Going 1 step further, we introduced SNPs in the coding sequences of both transporters and created single and double transfectant models to measure the relative importance of their respective activities and evaluate the importance of common genetic polymorphisms.

The principal observations that arose from our investigations are likely to be of importance because we (i) confirmed the implication of both the OATP2B1 influx and MRP1 efflux transporters in the cellular disposition of ATV, (ii) demonstrated that MRP1 efflux activity counteracts the ATV influx generated by OATP2B1, and (iii) showed that both investigated SNPs rs12422149 and rs45511401 affect the transporter activity toward ATV, with rs12422149 being

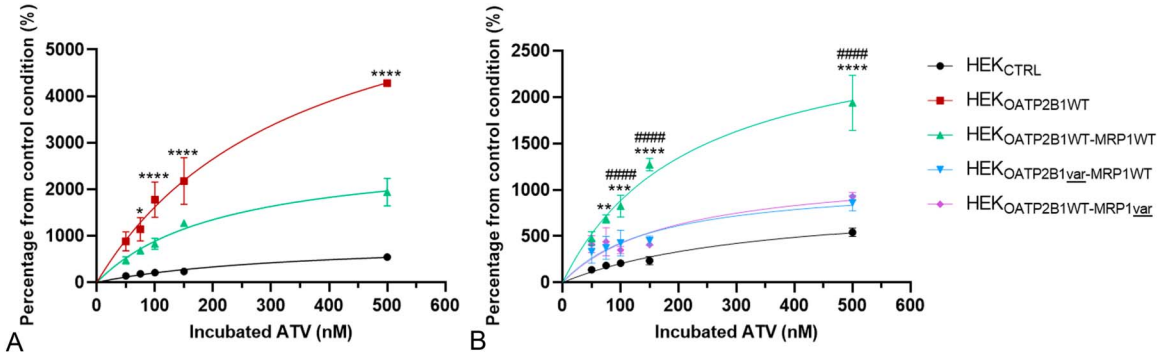

FIGURE 3. ATV accumulation experiment represented in percentage of accumulation from the control condition (ATV accumulation in HEK_{CTRL} at the lowest concentration) in (A) single transfectant $HEK_{OATP2B1WT}$ versus double transfectant $HEK_{OATP2B1WT-MRP1WT}$ and versus HEK_{CTRL} (*$P < 0.05$, ****$P < 0.0001$ compared with double transfectant WT model) and in (B) double WT transfectant versus variant models (**$P < 0.01$, ***$P < 0.001$, ****$P < 0.001$ compared with $HEK_{OATP2B1var-MRP1WT}$ model and #####$P < 0.0001$ compared with $HEK_{OATPWT-MRP1var}$).

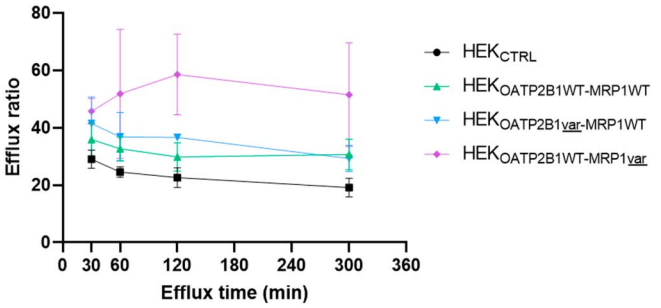

FIGURE 4. ATV efflux ratio in cell models from 30 to 300 minutes of efflux time. The efflux ratio is reporting the effluxed ATV amount in the media compared with the initial intracellular ATV amount, normalized on protein content. Nonsignificant results, $P > 0.05$ with Bonferroni post hoc tests.

associated with a lower OATP2B1 influx and rs45511401 with a higher MRP1 efflux.

In single transfectant models, we showed that OATP2B1 overexpression increased intracellular ATV accumulation, confirming its role in ATV cellular trafficking. We also observed that rs12422149 decreased this boosting effect, suggesting a defective effect on its activity. Second, our results in double transfectant models demonstrated that MRP1 efflux activity reduces the increased accumulation generated through OATP2B1 influx more effectively when the rs45511401 SNP was introduced in the *ABCC1* coding sequence. These observations suggest that the efflux activity of MRP1 seems to be boosted by the SNP because for a comparable OATP2B1 activity (OATP2B1WT), the accumulation was lower in $HEK_{OATP2B1WT\text{-}MRP1var}$ than in $HEK_{OATP2B1WT\text{-}MRP1WT}$. Efflux kinetics experiments corroborated the results of the accumulation experiments and consolidated our assumption of increased activity of the *ABCC1* variant (rs45511401). By contrast, the SNP introduced in the *SLCO2B1* coding sequence seemed to decrease the OATP2B1 influx activity because for a comparable MRP1 activity (MRP1WT), the accumulation in $HEK_{OATP2B1var\text{-}MRP1WT}$ was lower than that in $HEK_{OATP2B1WT\text{-}MRP1WT}$. This observation also confirmed the results obtained in the single transfectant model with $HEK_{OATP2B1WT}$ and $HEK_{OATP2B1var}$.

The observation that ATV is being transported by the influx protein OATP2B1 is in accordance with Grube et al.[24] Concerning the effect of the rs12422149 *SLCO2B1* SNP, to the best of our knowledge, this is the first study evaluating the effect of this SNP on the activity of the transporter toward ATV either in vitro or in vivo. When considering other statins, in a mixed cohort of 34 healthy individuals and 40 patients, Tsamandouras et al[20] showed that the rs12422149 SNP in *SLCO2B1* was associated with an increased apparent simvastatin acid clearance using population PK modeling. The authors concluded that this missense polymorphism may be linked to a lower distribution of simvastatin acid in OATP2B1-expressing tissues, explained by a decreased OATP2B1 influx leading to a paradoxically higher elimination rate. Along the same lines, Kim et al[21] highlighted in 2017 that among 18 volunteers, carriers of the rs12422149 *SLCO2B1* SNP, rosuvastatin was less effective in reducing LDL cholesterol after 8 weeks of treatment ($P = 0.012$). This could be explained by reduced OATP2B1 influx transport of the drug into hepatocytes, leading to reduced efficacy of rosuvastatin and increased levels of the drug in the blood circulation. It is important to stress that OATP2B1 has higher expression levels in the liver than in the muscle and is also expressed at lower levels in the lungs and placenta. However, to the best of our knowledge, OATP2B1 is the only ATV influx transporter expressed in skeletal muscle tissue. Considering the large tissue distribution, the consequences of this SNP at the systemic level are difficult to predict. On one hand, a decreased distribution of the drug in peripheral tissues where the protein is expressed (eg, the skeletal muscle and the lungs) is expected. On the other hand, the decreased OATP2B1 influx activity in hepatocytes would reduce the hepatic uptake and, consequently, the active fraction along with drug clearance,[4] leading to a higher systemic exposure in all cases. However, it is important to stress that in hepatic tissue, other influx transporters known to be implicated in the hepatic uptake of statins, such as OATP1B1 or 1B3, can eventually compensate for the decreased OATP2B1 activity. As a consequence, given the lack of OATP1B1 and OATP1B3 expression in the skeletal muscle tissue, one can speculate that the functional defect caused by this SNP would have a greater impact on local exposure (ie, in the myocytes) where no other influx transporters can compensate for the consequent decreased influx activity than on the systemic clearance, where other transporters can compensate for this decreased influx activity.[25] Therefore, we showed that in an isolated model of OATP2B1 overexpression, this SNP was associated with reduced cellular influx of ATV, suggesting a theoretical protective effect of these SNPs on the risk of atorvastatin cellular accumulation and possibly muscle symptoms.

We also highlighted that the rs45511401 SNP (c.2012G > T) in *ABCC1* was associated with an apparent increase in efflux activity of MRP1 against ATV using our double transfectant models, suggesting that this SNP could protect against ATV intracellular accumulation. By contrast, in the single transfectant MRP1 model, no effect of MRP1 efflux on ATV accumulation was observed, except at high concentrations (see **Supplemental Data, Figure S2**, **Supplemental Digital Content 1**, http://links.lww.com/TDM/A619). This may be because the affinity (Km) of the transporter is too low and requires prior activity of an influx of drugs to assess its implication in drug transportation. This observation agrees with the in vitro study of Knauer et al, which showed that the impact of MRP1 activity is significant only when coexpressed with rodent-Oatp2b1.[12] Few data are available regarding the impact of this *ABCC1* SNP on ATV transport. Nevertheless, in 2017, Behdad et al reported a study of 179 patients with primary hypercholesterolemia related to the impact of rs45511401 in *ABCC1* and rs1045642 in *ABCB1* on clinical response to ATV. The investigation did not reveal any significant difference in lipid-lowering response when comparing patients expressing the *ABCC1* wild-type or variant genotype.[26] As for OATP2B1, the lack of a significant effect on systemic exposure and on the LDL cholesterol lowering

effect does not exclude a local PK effect because the protein is more importantly expressed in peripheral tissues, especially in the skeletal muscle tissue. Transcriptomic data revealed an *ABCC1* relative mRNA expression level of 1.552 transcripts per million in the liver, whereas levels were 10-fold higher in the skeletal muscle (15.65 transcripts per million), arguing in the sense of a pronounced local rather than a systemic effect (GTEx Portal).[27] To the best of our knowledge, no study has evaluated the impact of both SNPs, either in *ABCC1* or in *SLCO2B1* on the susceptibility to ATV-related muscle side effects.

Although this study helps to clarify the impact of transporter overexpression on ATV cellular accumulation and the impact of common SNPs in an isolated cellular HEK293 system, it does not consider (1) the impact of transporters at their physiological level of expression and (2) the impact of the expression of other transporters in a multicompartmental system (ie, the body). In fact, even if, among the transporters implicated in ATV PK, OATP2B1, and MRP1 are the most expressed in the muscle tissue, it does not exclude the possibility that the activity of other transporters affecting systemic PK could have an indirect effect on local muscle exposure. It is well known that other transporters, especially OATP1B1 and OATP1B3, can drive the transport of ATV and are predominant in ruling the systemic PK through hepatic uptake, highlighting that the physiological situation is much more complex than our in vitro model. Furthermore, similar experiments with ATV lactone are warranted, as even if controversial, some studies have reported lactone-associated muscle toxicity.[28]

CONCLUSIONS

Overall, our results consistently demonstrate that the intracellular PK of ATV is governed by the local expression and activity of drug transporters and that OATP2B1 and MRP1 are likely to play a significant role in this bidirectional dynamic. We showed that MRP1 efflux activity against ATV protects against its high accumulation generated through OATP2B1 influx. This observation may be linked to the protection against ATV-related toxicity at the skeletal muscle tissue level. We also showed that SNPs present in the coding sequences of these transporters may affect their activity and modulate the intracellular accumulation of their substrates, which may be associated with susceptibility to muscle discomfort. These results constitute the first step in the understanding of interindividual variability in ATV PK that could explain individual susceptibilities to muscular side effects.

ACKNOWLEDGMENTS

The authors wish to thank Mr Dauguet Nicolas and Prof Van der Smissen (CYTF and CELL/DDUV UCLouvain) for their outstanding assistance with the use of the FACS and fluorescence microscopy platforms, respectively.

REFERENCES

1. Adams SP, Tsang M, Wright JM. Lipid lowering efficacy of atorvastatin. *Cochrane Database Syst Rev*. 2012;12:Cd008226.
2. Jacobson TA, Schein JR, Williamson A, et al. Maximizing the cost-effectiveness of lipid-lowering therapy. *Arch Intern Med*. 1998;158: 1977–1989.
3. Bruckert E, Hayem G, Dejager S, et al. Mild to moderate muscular symptoms with high-dosage statin therapy in hyperlipidemic patients–the PRIMO study. *Cardiovasc Drugs Ther*. 2005;19:403–414.
4. Stillemans G, Paquot A, Muccioli GG, et al. Atorvastatin population pharmacokinetics in a real-life setting: Influence of genetic polymorphisms and association with clinical response. *Clin Translational Sci*. 2022;15:667–679.
5. Thompson PD, Panza G, Zaleski A, et al. Statin-associated side effects. *J Am Coll Cardiol.* 2016;67:2395–2410.
6. Baker SK. Molecular clues into the pathogenesis of statin-mediated muscle toxicity. *Muscle Nerve*. 2005;31:572–580.
7. Sakamoto K, Honda T, Yokoya S, et al. Rab-small GTPases are involved in fluvastatin and pravastatin-induced vacuolation in rat skeletal myofibers. *Faseb J*. 2007;21:4087–4094.
8. Morikawa S, Murakami T, Yamazaki H, et al. Analysis of the global RNA expression profiles of skeletal muscle cells treated with statins. *J Atheroscler Thromb*. 2005;12:121–131.
9. Norata GD, Tibolla G, Catapano AL. Statins and skeletal muscles toxicity: from clinical trials to everyday practice. *Pharmacol Res*. 2014;88: 107–113.
10. Ownby SE, Hohl RJ. Farnesol and geranylgeraniol: prevention and reversion of lovastatin-induced effects in NIH3T3 cells. *Lipids*. 2002;37:185–192.
11. Lennernas H. Clinical pharmacokinetics of atorvastatin. *Clin Pharmacokinet*. 2003;42:1141–1160.
12. Knauer MJ, Urquhart BL, Meyer zu Schwabedissen HE, et al. Human skeletal muscle drug transporters determine local exposure and toxicity of statins. *Circ Res*. 2010;106:297–306.
13. Rosenberg MF, Mao Q, Holzenburg A, et al. The structure of the multidrug resistance protein 1 (MRP1/ABCC1). *J Biol Chem*. 2001;276: 16076–16082.
14. Choudhuri S, Klaassen CD. Structure, function, expression, genomic organization, and single nucleotide polymorphisms of human ABCB1 (MDR1), ABCC (MRP), and ABCG2 (BCRP) efflux transporters. *Int J Toxicol*. 2006;25:231–259.
15. Conseil G, Cole SP. Two polymorphic variants of ABCC1 selectively alter drug resistance and inhibitor sensitivity of the multidrug and organic anion transporter multidrug resistance protein 1. *Drug Metab Dispos*. 2013;41:2187–2196.
16. Nies AT, Niemi M, Burk O, et al. Genetics is a major determinant of expression of the human hepatic uptake transporter OATP1B1, but not of OATP1B3 and OATP2B1. *Genome Med*. 2013;5:1.
17. König J, Cui Y, Nies AT, et al. A novel human organic anion transporting polypeptide localized to the basolateral hepatocyte membrane. *Am J Physiology-Gastrointestinal Liver Physiol*. 2000;278:G156–G164.
18. Kullak-Ublick GA, Ismair MG, Stieger B, et al. Organic anion-transporting polypeptide B (OATP-B) and its functional comparison with three other OATPs of human liver. *Gastroenterology*. 2001;120:525–533.
19. Kinzi J, Grube M, Meyer Zu, Schwabedissen HE. OATP2B1—the underrated member of the organic anion transporting polypeptide family of drug transporters? *Biochem Pharmacol*. 2021;188:114534.
20. Tsamandouras N, Dickinson G, Guo Y, et al. Identification of the effect of multiple polymorphisms on the pharmacokinetics of simvastatin and simvastatin acid using a population-modeling approach. *Clin Pharmacol Ther*. 2014;96:90–100.
21. Kim TE, Shin D, Gu N, et al. The effect of genetic polymorphisms in SLCO2B1 on the lipid-lowering efficacy of rosuvastatin in healthy adults with elevated low-density lipoprotein. *Basic Clin Pharmacol Toxicol*. 2017;121:195–201.
22. Ensembl;2021. Available at: https://www.ensembl.org/Homo_sapiens/Variation/Population?db=core;r=11:75172032-75173032;v=rs12422149;vdb=variation;vf=168665315. Accessed June 1, 2022.
23. Ensembl; 2021. Available at: https://www.ensembl.org/Homo_sapiens/Variation/Population?db=core;v=rs45511401;vdb=variation. Accessed June 1, 2022.
24. Grube M, Köck K, Oswald S, et al. Organic anion transporting polypeptide 2B1 is a high-affinity transporter for atorvastatin and is expressed in the human heart. *Clin Pharmacol Ther*. 2006;80:607–620.

25. V Willrich MA, Kaleta EJ, Bryant SC, et al. Genetic variation in statin intolerance and a possible protective role for UGT1A1. *Pharmacogenomics*. 2018;19:83–94.
26. Behdad N, Kojuri J, Azarpira N, et al. Association of ABCB1 (C3435T) and ABCC1 (G2012T) polymorphisms with clinical response to atorvastatin in Iranian patients with primary hyperlipidemia. *Iranian Biomed J*. 2017;21:120–125.
27. GTExPortal.org. Bulk tissue gene expression for ABCC1 [web site] 2021. Available at: https://www.gtexportal.org/home/gene/ABCC1. Accessed December 8, 2021.
28. Skottheim IB, Gedde-Dahl A, Hejazifar S, et al. Statin induced myotoxicity: the lactone forms are more potent than the acid forms in human skeletal muscle cells in vitro. *Eur J Pharm Sci*. 2008;33:317–325.